

Transient reverse current phenomenon in a *p-n* heterojunction comprised of poly(3,4-ethylene-dioxythiophene):poly(styrene-sulfonate) and ZnO nanowall

Jongsun Maeng, Minseok Jo, Seok-Ju Kang, Min-Ki Kwon, Gunho Jo, Tae-Wook Kim, Jaeduck Seo, Hyunsang Hwang, Dong-Yu Kim, Seong-Ju Park, and Takhee Lee^{a)}
 Department of Materials Science and Engineering, Gwangju Institute of Science and Technology,
 Gwangju 500-712, Republic of Korea

(Received 23 June 2008; accepted 5 September 2008; published online 24 September 2008)

We report the characteristics of a *p-n* heterojunction diode comprised of a poly(3,4-ethylene-dioxythiophene):poly(styrene-sulfonate) (PEDOT:PSS) as the hole-conducting *p*-type polymer and *n*-type ZnO nanowall networks. ZnO nanowall networks were synthesized on a GaN/sapphire substrate without metal catalyst using hot-wall type metal organic chemical vapor deposition. The *p-n* heterojunction diodes of PEDOT:PSS/ZnO nanowall exhibited a space charge limited current phenomena at forward bias and a transient reverse current recovery when a sudden reverse bias was applied from the forward bias condition. The minority carrier lifetime was estimated to be $\sim 2.5 \mu\text{s}$. © 2008 American Institute of Physics. [DOI: 10.1063/1.2990225]

ZnO nanostructures such as nanowires, nanobelts, and nanowalls have attracted great interest due to their unique properties, including a wide direct bandgap of 3.37 eV and large exciton binding energy (~ 60 meV) for potential applications in optoelectronic devices.¹⁻⁴ In particular, nanoscale hybrid structures consisting of low dimensional inorganic components (such as nanowires) and organic components have recently attracted considerable attention due to the advantages of nanowires and organic materials, such as modified light-matter interaction, low cost spin-coating processing, and mechanical flexibility.⁵⁻⁸ Particularly, spin coating of organic components may result in better junction properties since physical and chemical stresses are much lower at the interface than with other processing techniques.⁵ Hybrid *p-n* junctions with *n*-type ZnO nanowires and *p*-type semiconducting polymers [poly(3,4-ethylene-dioxythiophene):poly(styrene-sulfonate) (PEDOT:PSS) or *N,N'*-di(naphtha-2-yl)*N,N'*-diphenylbenzidine] have shown possible applications as light emitting devices.⁶⁻⁸ Most studies in hybrid *p-n* junctions using ZnO nanowires and semiconducting polymer matrices focused on electroluminescence for photonic applications. However, the detail charge carrier dynamics of hybrid *p-n* junctions have not been thoroughly studied. For example, reverse recovery measurement can be done to estimate the minority carrier lifetime in organic/inorganic hybrid *p-n* junctions. Detailed study on the minority carrier dynamics will prove the formation of *p-n* junctions and enhance understanding the characteristics of *p-n* junctions.

In this study, we characterize a heterojunction diode comprised of *n*-type ZnO nanowall networks with a hole-conducting (*p*-type) polymer. We describe the reverse recovery switching characteristics after the *p-n* heterojunction diode was suddenly switched from forward to reverse bias. We synthesized the ZnO nanowall networks as *n*-type inorganic materials on a GaN/sapphire substrate without metal catalysts by metal organic chemical vapor deposition (MOCVD). Detailed knowledge of charge carrier dynamics is important

for understanding the transport properties of this *p-n* heterojunction diode and will be useful for future polymer/ZnO hybrid optoelectronic device applications.

ZnO nanowall networks were grown on an epitaxial GaN film ($\sim 2 \mu\text{m}$ thickness) on a *c*-plane sapphire substrate without metal catalysts using a hot-wall type MOCVD at a growth temperature of $\sim 800^\circ\text{C}$. To measure ZnO nanowall conductivity, ZnO nanowalls were dispersed in isopropyl alcohol by sonication and dropped on an oxidized silicon wafer. The conductivity of the ZnO nanowall networks was determined as ~ 1 S/cm from characteristic current-voltage (*I-V*) curves from detached ZnO nanowall flakes.

Figure 1(a) shows a typical field emission scanning electron microscopy (FESEM) image of a ZnO nanowall network. ZnO nanowall networks were grown perpendicular to the GaN (0001) film/*c*-plane sapphire substrate. A tilt view FESEM image of a ZnO nanowall network is shown in the

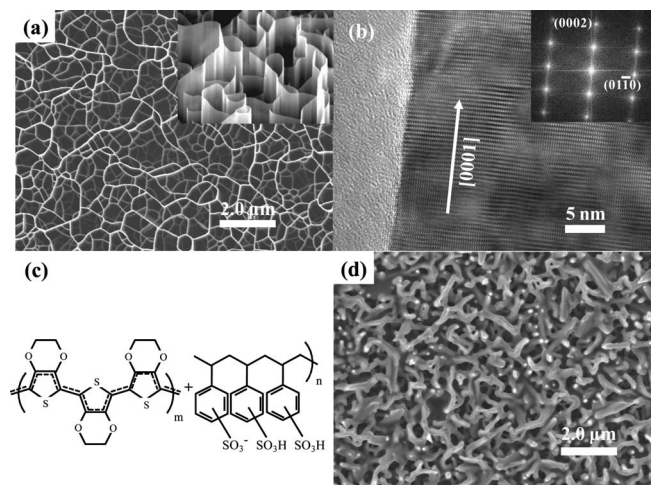


FIG. 1. (a) FESEM image of grown ZnO nanowall networks. Inset is a FESEM tilt image of the same ZnO nanowall networks. (b) Cross-sectional HRTEM image of a ZnO nanowall. Inset is the FFT pattern showing the $[2\bar{1}\bar{1}0]$ zone axis. (c) Molecular structures of PEDOT (left) and PSS (right). (d) FESEM image of ZnO nanowall networks after spin-coating with PEDOT:PSS.

^{a)}Electronic mail: tlee@gist.ac.kr.

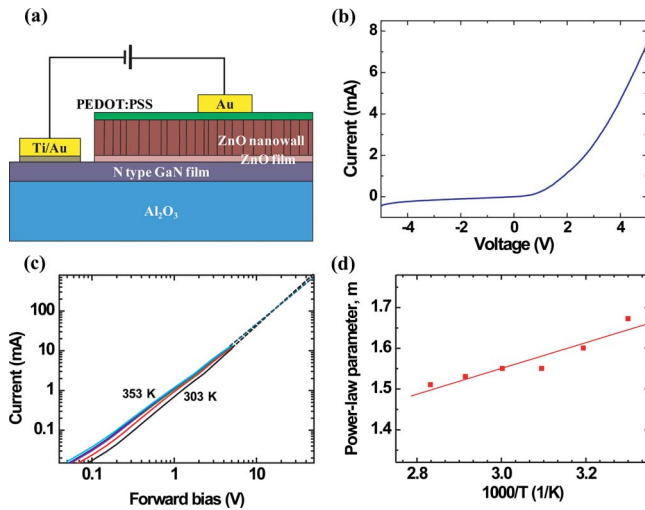


FIG. 2. (Color online) (a) Schematic diagram of the PEDOT:PSS/ZnO nanowall network p - n heterojunction on a ZnO thin film/GaN/ c -plane sapphire substrate. (b) Electrical characteristics of a PEDOT:PSS/ZnO nanowall network p - n heterojunction diode. (c) Temperature dependent I - V (log-log scale at forward bias) curves from 303 to 353 K by 10 K step. (d) The power-law parameter m obtained from (c) vs $1000/T$.

inset of Fig. 1(a). A ZnO thin film was formed prior to the growth of ZnO nanowalls, as reported previously.⁴ The nanowall thickness was found to be 20–50 nm and the size of a single domain was 100–500 nm. Figure 1(b) shows a high resolution transmission electron microscopy (HRTEM) image obtained from a ZnO nanowall cross section. This TEM image and the fast Fourier transform (FFT) pattern [inset of Fig. 1(b)] indicate a single crystalline phase with preferred growth in the [0001] direction in a $[2\bar{1}\bar{1}0]$ zone axis. The ZnO nanowall network was then spin coated with PEDOT:PSS (Baytron P VPAI 4083, purchased from H. C. Starck) from a 0.45 μm filtered aqueous solution, followed by drying at 120 $^{\circ}\text{C}$ for 10 min in ambient air. The typical spin coating rate was ~ 2000 rpm, and the film thickness of PEDOT:PSS was found to be ~ 40 nm. The conductivity of the p -type PEDOT:PSS films on a glass substrate was determined to be $< \sim 10^{-3}$ S/cm from four point measurements. The chemical structure of PEDOT:PSS is shown in Fig. 1(c).⁵ Figure 1(d) shows a FESEM image of nanowall networks after PEDOT:PSS spin coating.

A schematic of the PEDOT:PSS/ZnO nanowall network p - n heterojunction diode is shown in Fig. 2(a). The Ti (50 nm)/Au (50 nm) contact on the GaN film was formed, and the Au contact with a 400 μm box structure was deposited on the PEDOT:PSS surface by an electron-beam evaporator through a shadow mask. Figure 2(b) shows a typical I - V curve exhibiting p - n junction rectification behavior.

The forward bias current in conventional semiconductor diode is expressed as $J \propto \exp(qV/nk_B T)$ for $V > k_B T/q$, where q is elementary charge, V is the applied voltage, n is ideality factor, k_B is Boltzmann's constant, and T is the temperature. From the curve fitting of I - V characteristic in Fig. 2(b), an ideality factor n of ~ 96 was extracted. This high ideality factor suggests that the I - V characteristic of our device is not limited by forward bias current behavior of the conventional p - n junction, but rather by the carrier transport through PEDOT:PSS material. This indicates that the charge traps in PEDOT:PSS influence the electronic conduction through the device. This is called space charge limited current (SCLC)

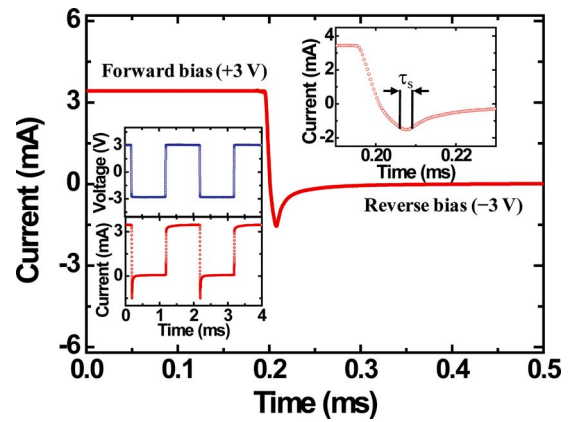


FIG. 3. (Color online) Reverse recovery characteristics after switching from forward (+3 V) to reverse bias (–3 V). Left inset shows the reverse current response by a series of pulses. Right inset is a magnified graph in the transition region used to estimate the carrier storage time (τ_s).

conduction, a well-known conduction model for the cases when there are a low free carrier density and a large trap density in conducting materials. The I - V characteristics in “trap-limited” SCLC model was generally explained by “exponentially distributed traps.”^{9,10} Here, the exponentially distributed traps means traps are distributed exponentially in energy as $\exp(-E/k_B T_C)$, where E is energy measured from the bottom of conduction band or the top of valence band for n -type and p -type materials, respectively, and T_C is a characteristic temperature constant of the trap distribution. The term trap-limited means that the current is controlled by the traps via thermally activated carriers. In trap-limited SCLC conduction, the current behaves as $I \propto V^m$, where $m(=T_C/T + 1)$ is an exponent parameter.^{9,10} The exponentially distributed traps in polymer may arise from hydrogen- and oxygen-induced defects, which disrupt the π electron system by the addition of H or OH in aromatic molecular solids such as PEDOT:PSS and pentacene.¹¹ The SCLC conduction model has also been explained for the conduction in organic-inorganic hybrid materials as well. For example, Nadarajah *et al.* have reported that the forward current follows the $I \propto V^2$ relationship as a typical feature of SCLC in PEDOT:PSS/vertically oriented ZnO nanowires.⁷ Also, Kaya *et al.* have reported $I \propto V^m$ for polyaniline/Si heterojunction.¹²

In order to explain the trap limited SCLC conduction model more clearly, we measured temperature-variable current-voltage $I(V, T)$ characteristics, which is a widely used technique to investigate the conduction mechanism of the electronic transport properties. Figure 2(c) shows a log-log plot of current versus voltage (forward bias) while the temperature was varied from 303 to 353 K. The m parameters were determined from curve fittings of the data in Fig. 2(c) and found to decrease from 1.7 to 1.5 as the temperature was increased from 303 to 353 K, as plotted in Fig. 2(d). The reduction of the parameter m as increasing temperature is consistent with the trap-limited SCLC conduction model.^{9–15}

Figure 3 shows typical reverse recovery characteristics of the PEDOT:PSS/ZnO nanowall network p - n heterojunction diode when it is suddenly switched from forward (+3 V) to reverse bias (–3 V). A series of 6 V square wave voltage pulses with a 1 ms pulse duration were applied and the current response was simultaneously recorded in an oscilloscope. In the bipolar p - n junctions, minority carriers can be stored when the diode is forward biased, and a large tran-

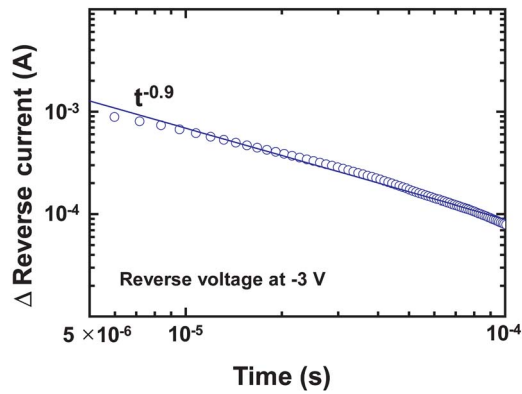


FIG. 4. (Color online) The log-log plot of reverse current variation at a reverse voltage of -3 V.

sient reverse current is required to extract carriers when the device is switched to reverse bias.^{16–18} The lifetime τ_n of the minority carriers (electrons in PEDOT:PSS layer in our case) can be expressed as

$$\tau_n = \frac{\tau_s}{\ln\left(1 + \frac{I_F}{I_R}\right)}, \quad (1)$$

where τ_s is the carrier storage time, I_R (~ 1.54 mA) is the maximum reverse current during the storage time period (at -3 V), and I_F (~ 3.43 mA) is the forward current (at $+3$ V).¹⁸ A τ_s of ~ 3 μ s was determined as the time taken for the current to decay from the maximum reverse current to 10% of its original value, as shown in the right inset of Fig. 3. Equation (1) assumes that the ZnO nanowall conductivity (~ 1 S/cm) is much greater than that of p -type PEDOT:PSS ($< 10^{-3}$ S/cm), so that the current due to minority carriers (electrons) in the PEDOT:PSS junction is approximately the total current in the reverse bias condition.¹⁷ Then, the carrier lifetime τ_n can be calculated as ~ 2.5 μ s from Eq. (1). The carrier lifetimes for other devices have also been reported; for example, ~ 1 ms or higher for amorphous/crystalline Si p - n junctions, 1 μ s to 10 ns (as a function of doping concentration) for crystalline Si p - n junctions and ~ 40 ns for GaN p - i - n rectifiers have been reported.^{17,19,20} As compared with crystalline p - n homojunctions, the relatively long minority carrier lifetime in our p - n heterostructure diodes is due to the trap-limited carriers in PEDOT:PSS.^{19–21} Note that the recovery time is defined as the time required for the reverse current to reach 10% of the reverse current saturation value and was estimated to be ~ 700 μ s in our devices.

Figure 4 presents a log-log plot of reverse current reduction [$\Delta I = I(\text{saturated}) - I(t)$] from 5 μ s after the maximum reverse current to 0.1 ms, which were chosen to eliminate the carrier storage effect after switching to reverse bias. The reverse current variation follows a form of $\Delta I \propto t^{-\gamma}$ with a factor γ of ~ 0.9 at a reverse bias of -3 V.²² The γ factor in the transient currents has been reported to be ~ 0.25 and ~ 0.5 for amorphous Si Schottky diodes and amorphous Si p - i - n

diodes, respectively.²² These power-law behaviors may be associated with an exponential distribution in energy of the trap states due to structural disorders in the amorphous Si junctions.²¹ Therefore, different trap states will behave with different power laws.²²

In summary, we studied the transient reverse current phenomena for a p - n heterojunction diode comprised of p -type PEDOT:PSS polymer and n -type ZnO nanowall networks. The PEDOT:PSS/ZnO nanowall heterojunction was observed to operate with space charge limited current in forward bias. The minority carrier lifetime of ~ 2.5 μ s was estimated from the reverse recovery characteristics. The results of our study may offer a fundamental understanding in the field of carrier dynamics, which may be useful for potential applications of hybrid ZnO nanowall network with organic materials.

This work was supported through the National Research Laboratory (NRL) program of the Korea Science and Engineering Foundation (KOSEF) and the Program for Integrated Molecular System at GIST.

¹W. I. Park, G.-C. Yi, M. Kim, and S. J. Pennycook, *Adv. Mater. (Weinheim, Ger.)* **15**, 526 (2003).

²Z. R. Dai, Z. W. Pan, and Z. L. Wang, *Adv. Funct. Mater.* **13**, 9 (2003).

³H. T. Ng, J. Li, M. K. Smith, P. Nguyen, A. Cassell, J. Han, and M. Meyyappan, *Science* **300**, 1249 (2003).

⁴S.-W. Kim, H.-K. Park, M.-S. Yi, N.-M. Park, J.-H. Park, S.-H. Kim, S.-L. Maeng, C.-J. Choi, and S.-E. Moon, *Appl. Phys. Lett.* **90**, 033107 (2007).

⁵M. Nakano, A. Tsukazaki, R. Y. Gunji, K. Ueno, A. Ohtomo, T. Fukumura, and M. Kawasaki, *Appl. Phys. Lett.* **91**, 142113 (2007).

⁶C.-Y. Chang, F.-C. Tsao, C.-J. Pan, G.-C. Chi, H.-T. Wang, J.-J. Chen, F. Ren, D. P. Norton, and S. J. Pearton, *Appl. Phys. Lett.* **88**, 173503 (2006).

⁷A. Nadarajah, R. C. Word, J. Meiss, and R. Könenkamp, *Nano Lett.* **8**, 534 (2008).

⁸X. W. Sun, J. Z. Huang, J. X. Wang, and Z. Xu, *Nano Lett.* **8**, 1219 (2008).

⁹A. Rose, *Phys. Rev.* **97**, 1538 (1955).

¹⁰P. Mark and W. Helfrich, *J. Appl. Phys.* **33**, 205 (1962).

¹¹M. Arif, M. Yun, S. Gangopadhyay, K. Ghosh, L. Fadiga, F. Galbrecht, U. Scherf, and S. Guha, *Phys. Rev. B* **75**, 195202 (2007).

¹²M. Kaya, H. Çetin, B. Boyarbay, A. Gök, and E. Ayyıldız, *J. Phys.: Condens. Matter* **19**, 406205 (2007).

¹³M. M. A.-G. Jafar, *Semicond. Sci. Technol.* **18**, 7 (2003).

¹⁴H. W. Lau, O. K. Tan, and D. A. Trigg, *Appl. Phys. Lett.* **89**, 113119 (2006).

¹⁵D. S. Chung, D. H. Lee, C. Yang, K. Hong, C. E. Park, J. W. Park, and S.-K. Kwon, *Appl. Phys. Lett.* **93**, 033303 (2008).

¹⁶Y. Zhou, M. Li, D. Wang, C. Ahyi, C.-C. Tin, J. Williams, M. Park, N. M. Williams, and A. Hanser, *Appl. Phys. Lett.* **88**, 113509 (2006).

¹⁷Y. Irokawa, B. Luo, J. Kim, J. R. LaRoche, F. Ren, K. H. Baik, S. J. Pearton, C.-C. Pan, G.-T. Chen, J.-I. Chyi, S. S. Park, and Y. J. Park, *Appl. Phys. Lett.* **83**, 2271 (2003).

¹⁸H. J. Kuno, *IEEE Trans. Electron Devices* **11**, 8 (1964).

¹⁹M. Nath, P. Chatterjee, J. Damon-Lacoste, and P. R. Cabarrocas, *J. Appl. Phys.* **103**, 034506 (2008).

²⁰C. H. Wang, K. Misiakos, and A. Neugroschel, *IEEE Trans. Electron Devices* **37**, 1314 (1990).

²¹T. Offermans, S. C. J. Meskers, and R. A. J. Janssen, *Org. Electron.* **7**, 213 (2006).

²²R. I. Hornsey, K. Aflatooni, and A. Nathan, *Appl. Phys. Lett.* **70**, 3260 (1997).